Exciton dynamics in single-walled nanotubes: Transient photoinduced dichroism and polarized emission

C.-X. Sheng and Z. V. Vardeny*
Department of Physics, University of Utah, Salt Lake City, Utah 84112, USA

A. B. Dalton and R. H. Baughman
Nano Tech Institute, University of Texas at Dallas, Richardson, Texas 75083, USA
(Received 19 May 2004; revised manuscript received 31 August 2004; published 28 March 2005)

Ultrafast relaxation of photoexcitations in semiconducting single-walled carbon nanotubes (*S*-NTs) were investigated using polarized pump-probe photomodulation (with 150 fs time resolution) and cw polarized photoluminescence (PL). Both annealed and unannealed thin NT films and D_2O solutions of isolated NTs were investigated. Various transient photoinduced bleaching (PB) and photoinduced absorption (PA) bands, which show photoinduced dichroism, were observed in the ultrafast photomodulation spectra of all NT forms. The PA and PB decay dynamics as a function of time, t, follow a power law, $(t)^{-\alpha}$ with α in the range of 0.7 to 1. Whereas the PA bands in *S*-NTs in solution uniformly decay, the PB bands, in contrast, have different decay dynamics across the spectrum, which originates from an ultrafast spectral shift. Nevertheless the dynamics of the PA and PB bands for NTs in solution are the same when the spectral shift is accounted for, indicating a common origin. In addition *S*-NTs in D_2O solution show polarized PL emission bands in the mid infrared spectral range that follow almost exactly the infrared absorption peaks of the isolated NTs, as well as their transient PB spectrum. The PL emission shows a degree of polarization that agrees with that of the transient photoinduced dichroism. We therefore conclude that the primary photoexcitations in *S*-NTs are not free carriers, rather they are *excitons* that are confined along the nanotubes. We found that the transient relaxation kinetics of the excitons depend on the NT form. The fastest exciton dynamics (with sub-picosecond lifetime) characterizes the annealed film, whereas the slowest dynamics (with lifetime of tens of ps) characterizes the isolated NTs in D_2O solution. From the polarization memory decay we could estimate the diffusion constant, D, and the diffusion length, L_D, of the excitons along the nanotube. For the annealed films at room temperature we found $D \approx 100$ cm^2 s^{-1} and $L_D \approx 100$ nm. From the average PL polarization degree, which remains constant across the PL spectrum, and the transient polarization memory decay, we estimate the PL lifetime in NT solution to be of the order of 500 ps. This relatively long PL lifetime is dominated by nonradiative decay processes, which when coupled with the minute PL emission quantum efficiency indicates a very small radiative recombination rate. The weak radiative transition strength is consistent with recent excited state calculations that include electron-hole interaction, which predict that excitons in NTs are basically dark.

DOI: 10.1103/PhysRevB.71.125427 PACS number(s): 78.47.+p, 72.20.Jv, 78.55.Kz, 78.67.Ch

I. INTRODUCTION

Carbon nanotubes (NTs) have very interesting mechanical[1] and electronic[2,3] properties, which have stirred the interest of many research groups during the past decade. Recently developed methods for spatially separating single-walled carbon NTs (SWCNTs) have enabled such basic optical studies as polarized absorption[4,5] and Raman scattering[6,7] on films of unbundled NTs. Photoluminescence (PL) emission has been observed for semiconducting *(S-)* NTs suspended in D_2O solutions[8,9] and for single isolated NTs.[7,10] Recently electroluminescence of single *S*-NT has been realized.[11,12] The PL emission measurements have refocused questions concerning the nature of the primary photoexcitations in *S*-NTs. In particular, the role of excitons in the optical spectra of *S*-NTs has been reinstated, since excitons are responsible for the measured PL.[8–10] Very good overlap was found between the measured bands in the optical absorption and those in the PL emission spectrum.[13,14] In addition, electron energy calculations on *S*-NTs (in which electron-electron and electron-hole interactions have been explicitly included) show a large exciton binding energy, in part because of the enhanced Coulomb interaction in these quasi-1D systems.[15–23] As a matter of fact, the results of the model calculations for excitons in NTs are similar to those of excitons in π-conjugated polymers, which also show large binding energies,[24–26] indicating that excitons in quasi-1D systems may have common properties.

Recent experimental studies of the nonlinear optical properties and photoexcitations dynamics in SWCNTs have demonstrated ultrafast kinetics, and therefore potential optoelectronic applications were proposed. For example, femtosecond (fs) time-resolved photoemission measurements were made on annealed metallic NTs (*M*-NTs), which show that the excited electron lifetime decreases from 130 fs at 0.2 eV to less than 20 fs at 1.5 eV above the Fermi energy.[27] Chen *et al.*[28] reported sub-picosecond relaxation kinetics of excited states in NT/π-conjugated-polymer composites at probe energy of 1.55 μm, which showed that NTs could be used for ultrafast switching in optical communication technology. It has also been shown[29] that resonant excitation of *S*-NTs enhances the third-order nonlinear optical coefficient,

$\chi^{(3)}$, which was found to be as high as 10^{-7} esu. Lauret *et al.*[30] discussed the recombination kinetics of photoexcitations in pump-probe measurements under resonant excitation conditions in *S*-NTs, which occurs on a 1 ps time scale. They observed photoinduced bleaching (PB) when pumping at or above the interband transitions, and photoinduced absorption (PA) when pumping at lower photon energies, which they attributed to the redshift of the global π-plasmon in the NTs. Our group[31] has recently reported transient photomodulation spectra of both *S*- and *M*-NTs using a low-repetition-rate, high-power ultrafast laser system that generated large photoexcitation densities of the order of $5\times10^{19}/\mathrm{cm}^3$. We found various PB and PA bands in *S*-NTs that are correlated with each other. From these findings, we concluded that the primary photoexcitations in *S*-NT are excitons rather than free carriers. In *M*-NTs, on the contrary, we showed that the primary photoexcitations are hot carriers. Ostojic *et al.*[32] have recently reported the transient photoexcitation kinetics of *S*-NTs in D_2O solutions, and showed that the decay kinetics is dependent on the solution PH.

Here we report ultrafast, time-resolved studies of photoexcitations dynamics of *S*-NTs in annealed and unannealed NT films, and for isolated NTs in D_2O solution, using a high-repetition-rate, low-power laser system that generates photoexcitation density of the order of 10^{16} cm^{-3}. The low photoexcitation density enabled us to study the intrinsic photoexcitation dynamics without the complication of exciton-exciton and/or pump-photon/exciton interactions, which characterize high power laser systems. For our studies we used the polarized pump and probe technique where the probe spans a variety of wavelengths in the mid infrared spectral range, using transient photomodulation (PM) spectroscopy with 150 fs time resolution.

We found that the transient PM spectra of all of the investigated nanotube samples contain PA and PB bands that are similar, but not exactly the same, as those found in our previous work for annealed NTs.[31] When taking into account the transient spectral shift that we observed in the PB bands, we conclude that the decay dynamics of the various bands in the transient PM spectrum characterize a common type of primary photoexcitation. In addition, the PM bands show transient photoinduced dichroism or polarization memory in all NT samples, where $(\Delta T/T)_{\parallel}\neq(\Delta T/T)_{\perp}$; here $\parallel$ and $\perp$ denote pump-probe polarization either parallel or perpendicular to each other, and $\Delta T/T$ is the fractional change ΔT in transmission, T. The prompt polarization memory, $P(t)$, decays at various rates depending on the form of the investigated NT sample and the excitation photon energy. The fastest decay was measured for NTs in annealed films, whereas the slowest decay was found for isolated NTs in D_2O solution. We found that the polarization memory is consistent with confined photoexcitations, so that the primary photoexcitations in NTs cannot be delocalized free carriers, as previously assumed.[28–30,32] We also measured PL emission for isolated NTs in D_2O solution and found it to have the same emission spectrum as the absorption and transient PB spectra; in addition, the PL is polarized. The PL polarization degree equals the transient photoinduced polarization memory that we measured at long times (of order of 1 ns). We therefore conclude that the primary photoexcitations in *S*-NTs are *excitons* rather than free carriers in continuum bands. From the minute PL quantum efficiency, the polarization memory decay in the transient response, and the polarization degree of the PL emission we estimate the radiative recombination time of NTs in solution to be 3 ± 2 μs.

We also found that the photoinduced exciton dynamics depend on the NT form; however the various photoinduced PB and PA bands are basically the same in all three types of NT samples. The exciton dynamics is fastest for the annealed samples and slowest for NTs in D_2O solution. The different exciton dynamics and polarization memory decays for the annealed and unannealed NTs, as well as for the NTs in D_2O solution, show that impurities and/or defects in the NTs have a profound influence on the electronic relaxation processes.

Since NTs are considered to be quasi-1D, the photoinduced polarization memory may be lost only when the photogenerated excitons diffuse along a bent NT so that their direction becomes random with respect to the polarization direction of the pump beam. From electron microscopy images we estimate the NT radius of curvature to be about 300 nm in the annealed NT films.[33,34] Using a model for the exciton diffusion along the bent NTs used before to estimate soliton diffusion in $t-(CH)_x$ (Ref. 35) we could estimate the exciton diffusion coefficient, D, from the polarization memory decay dynamics. We found $D\approx100$ $\mathrm{cm}^2\,\mathrm{s}^{-1}$ for *S*-NTs in the annealed film and much smaller for the unannealed film and for isolated NTs in D_2O solution.

II. EXPERIMENTAL

The single-walled carbon NTs used for these studies were prepared using the HiPco process and were supplied by CNI.[36] Typically, the raw material contains 85% wt % nanotubes and 15% iron catalyst nanoparticles. NTs were dispersed in H_2O or D_2O using the surfactant lithium dodecyl sulfate. Specifically, 0.4 wt % NTs were added to a 1.2 wt % LDS aqueous solution. Sonication was then performed using a VWR Scientific Branson Sonifier 250 with the sample immersed in an ice water bath. Samples were sonicated 20 min at a power level of 30 W, yielding dark black mixtures. Films were prepared by successive dip coating of glass substrates into the H_2O solutions. When the NT film is put in a chamber filled with argon gas and heated to 600 °C for 6 h, this annealing process removes most of the LDS. Otherwise the unannealed film is used as grown in our optical setup. From resonant Raman scattering measurements[37] we inferred that our samples contained *M*-NTs as well as *S*-NT with an approximate ratio of 1:2, having a diameter distribution from 0.7 to 1.4 nm with a peak distribution at a diameter of about 1.0 nm.

Dispersions of predominantly isolated nanotubes in D_2O were prepared using a procedure based on the method developed by O'Connell *et al.*[8] The sonicated samples were first centrifuged in an Eppendorf 5417C centrifuge for 10 min at $700\times$ g. The upper 75% of the supernatant was recovered using a small-bore pipette, avoiding sediment at the bottom, and transferred to a Beckman centrifuge tube for further centrifugation. Samples were then centrifuged for 2 h at $100,000\times$ g in a Beckman TL-100 ultracentrifuge with the

temperature controlled at 4 °C. The upper 50% of the supernatant was then recovered using a small-bore pipette, avoiding sediment at the bottom, and transferred to a clean tube. High-speed centrifugation sedimented insoluble NTs as a pellet, yielding homogeneous gray dispersions.

We used the fs two-color pump-probe correlation technique with linearly polarized light beams for the transient PM spectroscopy in the range between 0.55 and 1.05 eV. Our ultrafast laser system was a 100 fs titanium-sapphire oscillator operating at a repetition rate of about 80 MHz, which pumped an optical parametric oscillator (OPO) (Tsunami, Opal, Spectra-Physics) where both signal and idler beams were respectively used as probe beams. The pump beam was extracted either from the fundamental at $\approx$1.6 eV or from the signal beam at 0.93 eV. To increase the signal to noise ratio, an acousto-optical modulator operating at 85 KHz was used to modulate the pump beam intensity. For measuring the transient response at time t with $\approx$150 fs time resolution, the probe pulses were mechanically delayed with respect to the pump pulses using a translation stage; the time $t=0$ was obtained by a cross-correlation between the pump and probe pulses in a nonlinear optical crystal. Typically the pump intensity was kept lower than 5 μJ cm^{-2} per pulse, which corresponds to $\approx 10^{16}$ cm^{-3} initial photoexcitation density per pulse in the NT films. This density corresponds to less than a single photoexcitation per NT for the NTs in D_2O solution. The transient PM signal, $\Delta T/T(t)$ is the fractional change in transmission, T, which is negative for PA and positive for PB. The pump beam passed though a polarization rotator that changed its polarization to be 45° to that of the probe beam. An optical polarizer was used on the transmitted probe beam to analyze the changes of transmission, ΔT, for both parallel, $\Delta T_{\parallel}$, and perpendicular, $\Delta T_{\perp}$, polarizations.[22] The transient polarization memory, $P(t)=(\Delta T_{\parallel}-\Delta T_{\perp})/(\Delta T_{\parallel}+\Delta T_{\perp})$, was then calculated to study its decay. The pump and probe beams were carefully adjusted to get complete spatial overlap on the film, which was kept under dynamic vacuum. In addition the pump/probe beam-walk with the translation stage was carefully monitored and the transient response was adjusted by the beam walk measured response.

For the cw polarized PL emission study, we used the fundamental of the Ti-sapphire laser system at 1.6 eV operating at full power (1.5 W) to excite the isolated S-NT in the D_2O solution. The PL emission was collected by a lens with large F-number, and spectrally and spatially filtered to eliminate the relatively strong excitation laser intensity. A polarizer was used to select the PL emission either parallel or perpendicular to the polarization of the pump beam, and a polarization scrambler in front of the monochromator was used to detect the two PL components through the spectrometer. The collected PL emission was then directed onto the exit slit of a 1/4 m monochromator with 1 nm resolution; a nitrogen-cooled germanium photodiode was used for the light detection in the near and mid infrared spectral ranges. The PL spectrum was corrected for the background system response obtained when the NT solution was replaced by a solution from the same solvent that did not contain NTs.

III. RESULTS AND DISCUSSION

Typical optical absorption spectra, $\alpha(\omega)$, for the annealed and unannealed NT films and isolated NTs in solution are shown in Fig. 1. Absorption bands A, B, D in Fig. 1(a) for the NT films were previously assigned to the various inhomogeneously broadened interband optical transitions of the S-NTs in the sample. The absorption bands in this model are due to dipole-allowed symmetrical transitions from various valence subbands to their respective conduction subbands having the same index, m; namely, $m=\pm1$, ±2, and ±3, respectively. Band C, on the contrary, is the first interband transition ($m=\pm1$) of the M-NTs in the sample.[27,30] The absorption features related to the quasi-1D character of the NTs are more pronounced in the annealed sample, in agreement with the results of Itkis *et al.*,[38] suggesting that the annealing process purifies the NTs. This can be understood since the annealing process removes substituent groups that result from oxidation during nanotube purification. The background absorption in Fig. 1(a) was assigned to the absorption tail of the π-plasmon resonance (that peaks at about 5 eV), which does not change much as a result of annealing the film samples.[39] It is well known[3,30,32,39] that the absorption bands of M-NT appear at $\hbar\omega > 1.6$ eV and thus the S-NT in our films are preferentially excited by the pump pulses at $\hbar\omega = 1.55$ eV. However, the effect of the M-NT cannot be ignored in determining the energy relaxation routes in SWCNT films, where S-NT and M-NT are bundled together.

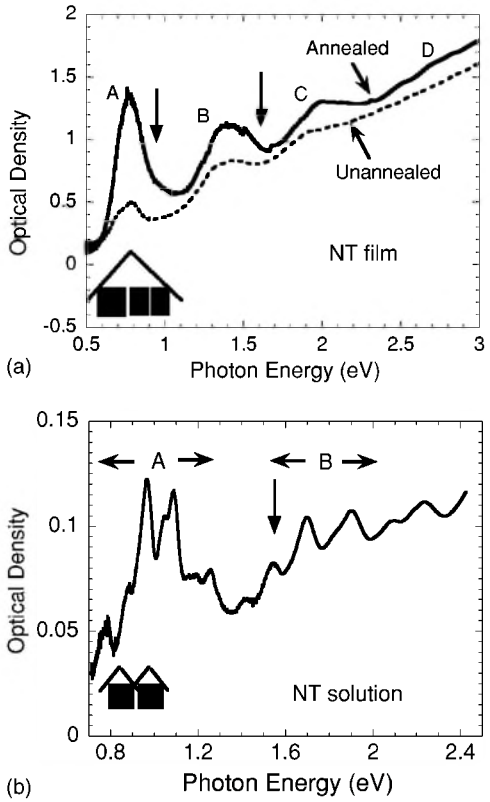

FIG. 1. Absorption spectra $\alpha(\omega)$ of SWCNTs in different forms. (a) Annealed (solid line) and unannealed (dashed line) NTs films, and (b) NTs in D_2O solution. The bands A, B and D are due to S-NT transitions; band C is due to M-NT transition. Black lines with arrow down (up) show pump (probe) photon energies used in this work.

In contrast with the SWCNT films, the absorption spectrum $\alpha(\omega)$ of NTs in D_2O solution [Fig. 1(b)] contains a

number of isolated subbands that belong to bands A, B, and C, respectively. This shows that the inhomogeneity of the NTs in D_2O solution is smaller than for the films; the NTs are probably bunched in more specific groups of NTs having the same diameter compared to those in films, and show less disorder. It is also noteworthy that the absorption background in $\alpha(\omega)$ is suppressed in the D_2O solution. This is surprising and calls for revisiting the explanation given for the absorption tail of NTs in NT films. When comparing Figs. 1(a) and 1(b), we note that peak A in films is at lower photon energy than the individual peaks in group A of the solution; also the bands marked B in the solution may in fact also contain peaks from band C in the films. Since the only difference between the NTs in films and solution is the NT isolation in the latter, the decrease in resonant energy shows either that the Van der Waals interaction in films is of the order of 0.2 eV, or that the exciton binding energy in NTs depends on the dielectric constant of the surrounding.[22] The different resonant energy of band A in films and solution presumably does not have a profound influence over the transient photoexcitation dynamics that is the focus of this work, since the pump photon energy is above band A in both cases. Also we expect that traps dominate the exciton dynamics;[31] in this case the exciton binding energy has little influence over the escape probability from the traps.[40] We also show in Fig. 1 the pump and probe photon energies used in this work; the arrows pointing down denote the various pump wavelengths, whereas the heavy arrows pointing up show the probe wavelengths.

In Fig. 2 we show the transient PM spectra of S-NTs in annealed film and D_2O solution in the mid infrared range at $t=0$. The PM spectra were generated with pump photon energy at 1.6 eV, which preferentially excites S-NTs; excitations in M-NTs are mainly photogenerated at 1.9 eV and higher.[27,30,31] This has also been derived from resonant Raman scattering studies.[3,41,42] The PM spectra contain both PB and PA bands and thus cannot originate from a shift in the global plasmon;[30] these are therefore photoinduced bands associated with specific optical transitions of the primary photoexcitations in S-NTs.[31] The PB bands in both films and solution are within the spectral range of band A in the respective absorption spectra (Fig. 1), and are thus due to either k-space state filling or Q-space filling, depending on whether carriers or excitons are photogenerated in S-NTs at $t=0$. From their similar dynamics and polarization memory decay it was previously concluded[31] that the transient PB and PA bands in the mid-ir spectral range are correlated, and thus the PA bands are due to optical transitions of photoexcitations that occupy electronic states associated with band A in the absorption spectrum. Note that the transient PB band is more structured for NTs in solution than for NTs in films, which agrees with the observation of more structure for the absorption subbands in the $\alpha(\omega)$ spectrum for the NTs in solution.

Figure 3 shows the uncorrected cw PL emission from the isolated S-NTs in D_2O solution plotted together with the transient PB spectrum [Fig. 2(b)] and $\alpha(\omega)$ in the same spectral range [Fig. 1(b)]. The PL is in fact a very weak emission band with estimated quantum efficiency of less than 10^{-3} [Refs. 8, 9, and 22]. It is apparent that the PL spectrum

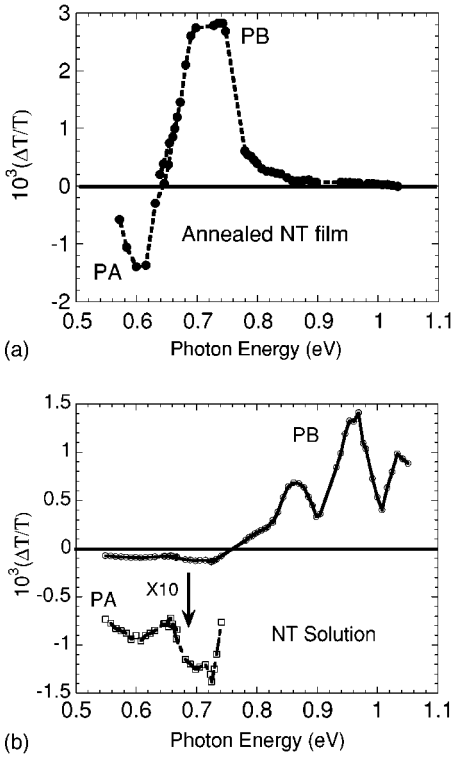

FIG. 2. Transient PM spectra measured at $t=0$ of annealed SWCNT film (a) and NTs in D_2O solution (b). Various PA and PB bands are assigned.

contains isolated emission subbands that are very similar to the absorption subbands in $\alpha(\omega)$; actually there is one-to-one correspondence between the PL and the absorption subbands. This shows that the subbands in $\alpha(\omega)$ are due to the same features that give PL emission. Due to their large binding energy compared to k_BT at room temperature, the PL in quasi-1D semiconductors originates from exciton emission.[24,40] The alternative explanation is that the PL emission is interband in origin.[8–10] If this were true, then the PL emission spectrum associated with each absorption band would have shown an asymmetric line shape towards higher photon energies;[43] which is not the case here (Fig. 3). We therefore conclude that the absorption subbands in $\alpha(\omega)$ are in fact *excitonic*. The obtained transient PB spectrum in D_2O

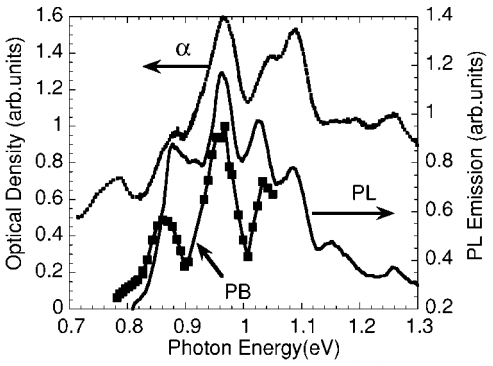

FIG. 3. Comparison between absorption $\alpha(\omega)$, PL emission, and transient PB spectra at $t=0$, for NTs in D_2O solution.

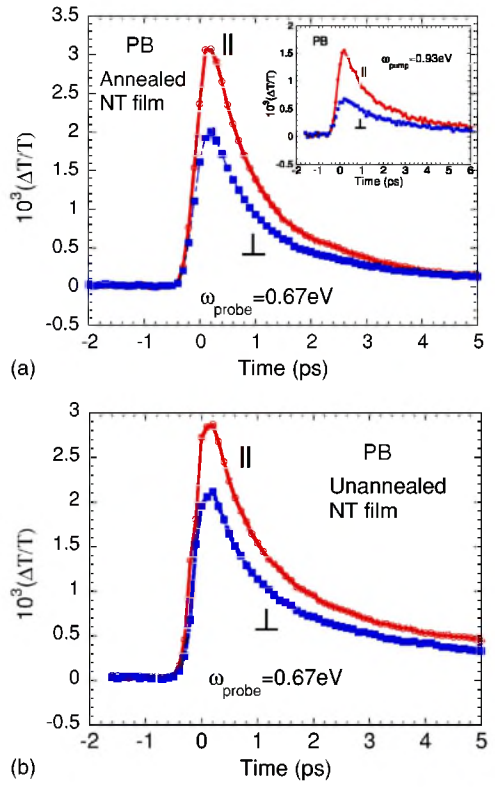

FIG. 4. (Color online) Transient polarized PB response at 0.67 eV for SWCNTs of different forms; both $\Delta T_{\parallel}$ and $\Delta T_{\perp}$ components are shown. (a) Annealed film excited with two different pump photon energies (see inset) and (b) unannealed film.

solution also follows the measured subbands in both $\alpha(\omega)$ and PL emission spectra. We thus infer that the primary photoexcitations that lead to the transient PB are *excitons*. This is in agreement with the conclusion drawn in our previous work,[31] which was based on the existence of inter-subband transitions (the PA bands in the transient PM spectrum), as well as the nonlinear optical response in *S*-NTs. It is worth noting that the observed dips and peaks in the PB spectrum (Fig. 3) are sharper than those obtained in the PL and $\alpha(\omega)$ spectra. This may be due to the nonlinear properties of the PB response. Whereas the PL emission and $\alpha(\omega)$ are linear optical processes, the PB response is a nonlinear optical process. In fact PB is related to the third-order optical nonlinearity, $\chi^{(3)}$, whereas $\alpha(\omega)$ and PL are related to $\chi^{(1)}$. It is known that, in general, the optical nonlinear spectra are much sharper than the corresponding linear spectra.

The exciton dynamics in the unannealed and annealed NT films were studied by measuring the transient polarized response for specific wavelengths within the PB bands, as shown in Fig. 4. The decay time constants of the obtained transient decays are summarized in Table I. The transient PA decays faster in the annealed film compared with that in the unannealed film. More specifically, the PA decay time constant, τ [defined as the time to reach $N(0)/3$, where $N(0)$ is the initial exciton density], is about 1 ps in the annealed film [Fig. 4(a)], compared with τ=2 ps for the unannealed film [Fig. 4(b)], (see Table I). The slower dynamics in the unannealed film is probably due to excess disorder that may give

TABLE I. The decay time constants, τ for the transient photomodulation response and τ' for the polarization memory decay, in various SWCNT films. A stands for annealed films; U is for unannealed films; and S is for NTs in D_2O solution. τ is defined as the time (in ps) for the initial response, $\chi^{(3)(0)}$ to decay to a third of its value, i.e., $1/3\chi^{(3)(0)}$, whereas τ' in films is derived from an exponential fit to the polarization memory decay. Note, however, that the PM decay curves have long tails due to their power law functional dependence.

Type	Pump energy (eV)	Probe energy (eV)	PM style	PM decay time τ (ps)	Polarization memory decay time τ' (ps)
U	1.6	1.6	PA	2.3	>6
A	1.6	1.6	PA	0.8	2.5
U	1.6	0.96	PB	2	>5
A	1.6	0.96	PB	0.6	~2
U	1.6	0.675	PB	2	>5
A	1.6	0.675	PB	1.2	3.4
U	0.96	1.6	PA	1.7	>6
A	0.96	1.6	PA	1.2	3.5
U	0.925	0.675	PB	4.2	>6
A	0.925	0.675	PB	1.7	2.2
S	1.6	1.01	PB	3	>10
S	1.6	0.97	PB	8	>60
S	1.6	0.83	PB	5	>60
S	1.6	0.66	PA	3	>60

rise to shallow traps that slow down the exciton recombination kinetics in this film.[44–46] Annealing heals defects and removes surfactants, which decreases the states due to shallow traps in the electronic density of states.[45] When excited within band *A* at 0.93 eV [Fig. 4(a) inset], then even the decay rate of the PA for the annealed film is slower, with τ =1.5 ps (Table I). This shows that the exciton dynamics is slower when excited resonantly, in agreement with recent measurements of Ostojic *et al.*[32]

The decay of PB for NTs in D_2O solution is much slower compared to that for NT films (Fig. 5). In addition, it seems that the decay dynamics changes across the PB spectrum. At ω_{probe}=1.01 eV, which is close to a dip in the PB and $\alpha(\omega)$ spectra (Fig. 3), we obtained for the PB decay τ=3 ps [Fig. 5(a) and Table I], whereas at ω_{probe}=0.97 eV, which is at a maximum in both PB and $\alpha(\omega)$ spectra (Fig. 3), we obtained $\tau \approx 8$ ps [Fig. 5(a) and Table I], with a tail towards longer times. This indicates that NTs in solution are also subject to disorder and inhomogeneity, which might be due to the added surfactants used for obtaining NT dispersion in solution. This disorder results in states in the gap, or shallow traps that may decrease the exciton recombination rate.[44–46] The different decay dynamics across the PB spectrum can be more clearly seen in Fig. 6, where the transient PB spectrum is depicted. It is seen that the PB spectrum blueshifts with time for each absorption subband in $\alpha(\omega)$. Figure 6 inset summarizes the shift of the PB maximum photon-energy in the first peak at 0.87 eV versus time. It is seen that the PB

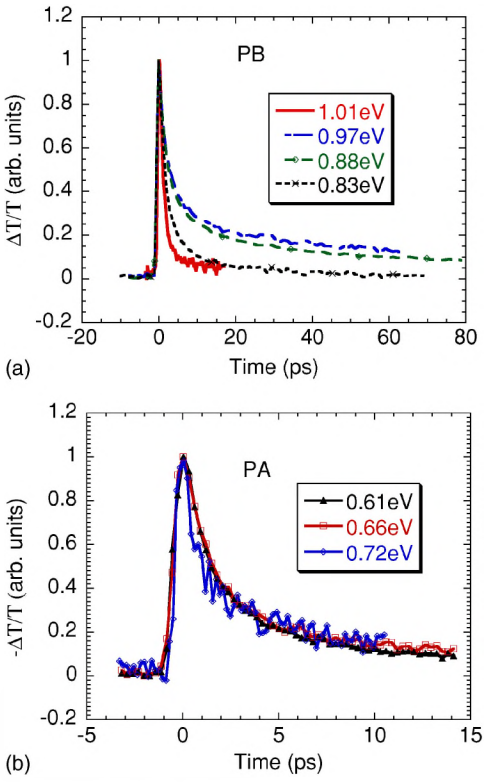

FIG. 5. (Color online) Transient polarized PM response of NTs in D_2O solution excited at 1.6 eV and probed at various photon energies within the PB bands (a) and PA bands (b).

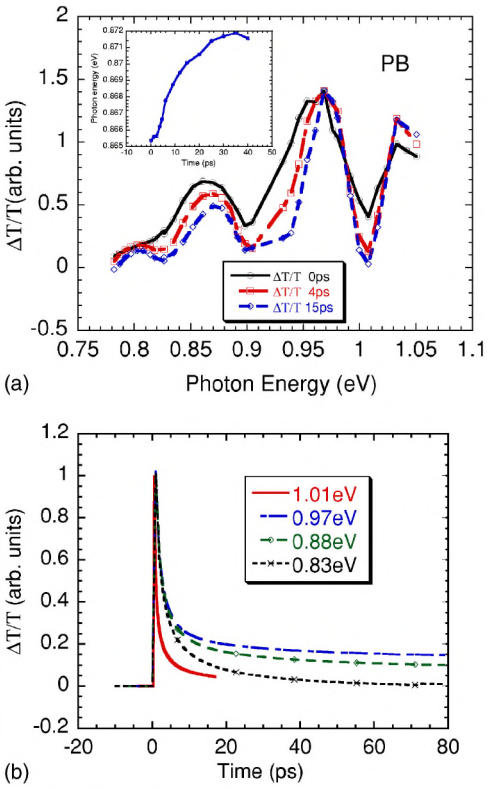

FIG. 6. (Color online) (a) Transient PB spectra of NTs in D_2O solution at three different times between the pump and probe pulses; the inset shows the peak position of the PB band at ≈0.85 eV at various times up to 40 ps. (b) The calculated transient decay of the PB band at various probe photon energies using the model described in the text.

maximum shifts with time by 7 meV in going from $t=0$ to $t=35$ ps; a similar spectral shift can be extracted from the second PB peak at 0.97 eV.

Such a spectral diffusion process does not occur in the PA bands [Fig. 5(b)], where a uniform time constant of about 3 ps (Table I) can be extracted from the data. Since the PA decay is simpler, we thus focus on its dynamics first. Figure 7(a) shows that in fact the PA decay is not exponential; instead, it is a power law of the form $(t/t_0)^{-\alpha}$, where $\alpha \approx 0.75$. The power law decay may originate either from dipressive transport type process[44–47] where the exciton diffusion constant towards recombination centers is time dependent,[28] or is due to a distribution of lifetimes, $g(\tau)$ having a tail towards longer time constants of the form $\tau^{-(1+\alpha)}$ and $\alpha \approx 0.75$.[48]

For analyzing the composite PB decay, we assume that there are two transient responses that occur simultaneously. One is a recombination process that has power law decay similar to the PA decay analyzed above, which can be described by the function $t^{-\alpha}$ with $\alpha=0.75$. The other transient process is a spectral diffusion, where the PB bands blueshift with time. The transient response across the PB spectrum can be therefore described by the following equation:

$$\mathrm{PB}_i(t) = C_{1,i}t^{-\alpha} + C_{2,i}[f_i(t) - f_i(0)], \qquad (1)$$

where PB_i is the response of each of the three subbands seen in the transient PB spectrum with index (i); $C_{1,i}$ and $C_{2,i}$ are constants, which are different for each subband (i); $\alpha=0.75$ is the exponent describing the dipressive recombination of both PA and PB responses; $f_i(t)$ describes the transient spectral shift (diffusion) of subband (i); and $f_i(0)$ is $f_i(t)$ at t=0. In Eq. (1) we describe $f_i(t)$ by the relation $f_i(t)=\exp\{-[E-E_{c,i}(t)^2]/2(\delta E)^2\}$, which is a Gaussian function centered at $E_{c,i}(t)$ having a width (δE), and E is the photon energy. At $t=0$ we obtained from the transient spectrum of the second PB subband at 0.96 eV [namely $i=2$ in Eq. (1)] δE=35 meV; for convenience we assume δE to be time independent and the same for all three obtained PB subbands. In our model we describe $E_c(t)$ shift with time by the equation

$$E_{c,i}(t) = E_{c,i}(0) + E_{d,i}[1 - \exp(-t/t_0)], \qquad (2)$$

where $E_{d,i}$ and t_0 are fitting parameters describing the average transient energy shift for the three PB subbands. The transient PB dynamics for all wavelengths were fit using Eqs. (1) and (2), and the best fitting parameters are summarized in Table II. We first let the peak maximum for all subbands shift exponentially with time with $t_0=13$ ps [Eq. (2)] that we obtained from the transient spectral shift in Fig. 6(a), whereas $E_{d,i}$ were left as fitting parameters (best fitting parameters given in Table II). Also the relative contribution of the two transient contributions to each PB subband, namely the decay due to recombination and the spectral shift, which

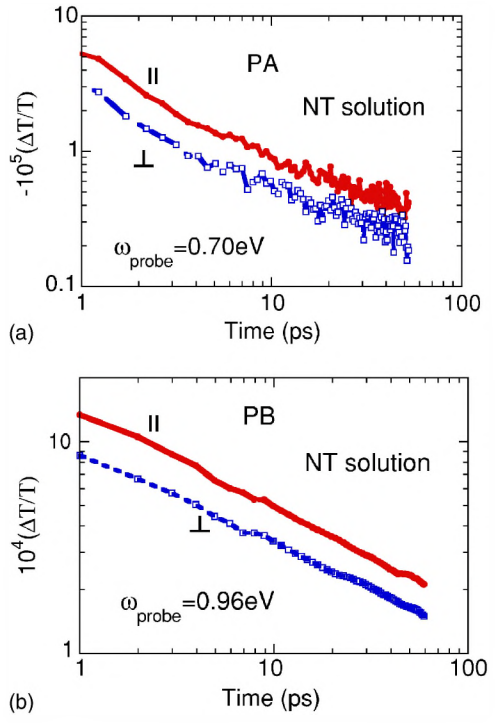

FIG. 7. (Color online) Transient polarized PM response of NTs in D_2O solution at various probes photon energies, where both $\Delta T_{\parallel}$ and $\Delta T_{\perp}$ components are shown (a) for the PA band and (b) for the PB band.

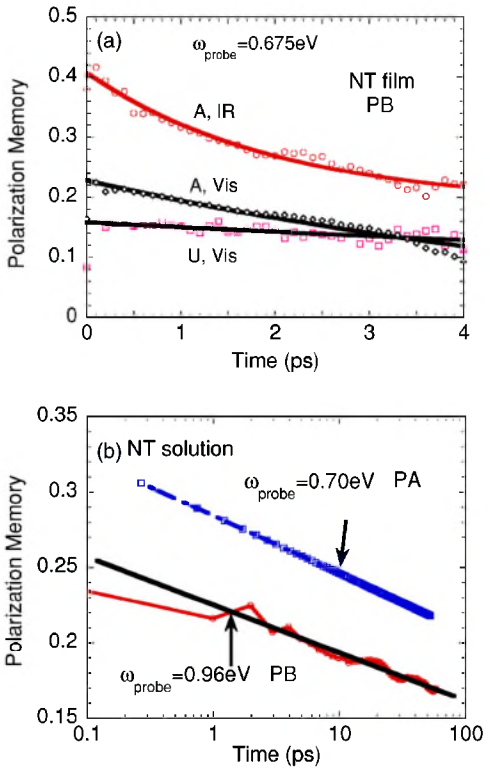

FIG. 8. (Color online) The polarization memory dynamics in SWCNTs of various forms. (a) Annealed (at two pump photon energies) and unannealed films at 0.675 eV (PB) and (b) NTs in solution at two different probe photon energies, at 0.96 (PB) and 0.70 eV (PA), respectively. Fitting lines through the data points for the polarization memory decay are also shown.

is given by the parameter $C_i = C_{2,i}/C_{1,i}$, were left as fitting parameters (Table II). The calculated decay curves for different photon energies using Eqs. (1) and (2) and the fitting parameters in Table II are shown in Fig. 6(b); they are in very good agreement with the experimental data shown in Fig. 5(a). Since the PB decay was fit with the same functional dependence as the PA decay, the agreement between the model calculation and experiment show that the PA and PB share a common underlying mechanism, and are in fact part of the same photoexcitation dynamics process.[31]

The most surprising transient response for the photogenerated excitons is their photoinduced polarization memory, where $\Delta T_{\parallel} \neq \Delta T_{\perp}$. Figure 4 shows the polarization memory in films, whereas Fig. 7 shows that polarization memory also exists for NTs in solution, for both PA and PB bands. A number of theoretical models for excitons in *S*-NTs have been recently developed.[15–23] These models put an upper limit for the exciton length at few nanometers, and also showed that the exciton is mainly polarized along the NT. Our experimental results are in agreement with these models. The obtained photoinduced polarization memory shows that excitons in NTs are indeed localized. Otherwise the polarization memory would have decayed within the pulse duration because the photogenerated excitations would simultaneously occupy the whole NT length, which is in fact isotropically bended.[33,34] The prompt polarization memory P(0) decays with time since the photogenerated excitons are quite mobile and thus may diffuse along the individual NT so that their induced dipole moment is no longer correlated with that at $t=0$ upon their generation (see the Appendix). The transient polarization memory $P(t)$ decays differently in the various NT forms, as summarized in Fig. 8. $P(0)$ is larger in the annealed film compared with that in the unannealed film [Fig. 8(a)]; it is also larger when excited with ir pump. The smaller P when excited in the visible spectral range shows that P is somewhat lost during the ultrafast exciton thermalization process from band B (in the visible) to band A (in the mid ir). Also $P(t)$ decays much slower in the unannealed film compared with $P(t)$ decay in the annealed film [Fig. 8(a)]. This suggests that the NT impurities change the polarization memory dynamics for NTs in the unannealed film. Exciton diffusion process along the NT is slower in this type of NT, probably because of the existence of shallow traps.[44,46] $P(t)$ dynamics in isolated NTs in solution [Fig. 8(b)] is very different from those in films [Fig. 8(a)]. First the decay is much

TABLE II. Fitting parameters for the PB decay in NTs in solution. $E_{c,i}(0)$ is the peak of the i's PB subband at $t=0$, whereas $C_i = C_{2,i}/C_{1,i}$ is the relative contribution of the spectral shift ($C_{2,i}$) to the recombination ($C_{1,i}$) dynamics [see text; Eq. (1)]. $E_{d,i}$ is the spectral diffusion energy due to the blueshift [see Eq. (2) in the text].

Peak energy $E_{c,i}(0)$(eV)	0.87	0.96	1.05
C_i	1.2	0.7	0.5
Spectral diffusion energy $E_{d,i}$(meV)	7	8	8

slower when measured at the peak energy of the PB band. Second $P(t)$ decays similarly for the PB or PA bands.

We may extract the exciton diffusion constant from the polarization memory decay using the "exciton diffusion around the corner" model presented in the Appendix. This model was previously used to obtain the diffusion constant of solitons in fibrils of trans-polyacetylene.[48] The eventual loss of polarization memory in the PM response is due to exciton diffusion along the bent NTs over sufficiently large distances so that the excited tubes' directions are random with respect to the pump polarization. The sufficiently large distance is related to the NT radius of curvature, R. In this model (see the Appendix) $P(t)$ is given by $P(t)=P(0)\exp(-t/\tau_D)$, where $\tau_D=R^2/4D$, $P(0)$ is P at $t=0$, D is the exciton diffusion constant, and R is the NT average radius of curvature in the film. τ_D can be extracted from Fig. 8. It is about 3 ps for NTs in the annealed film, and much longer for the NTs in the unannealed film and solution. From the definition of τ_D and its value, and using $R=300$ nm from STM images of the NTs in similar films as ours,[33,34] we estimate D for excitons along the NT in the annealed film to be $D\approx 100\pm 50$ cm^2 s^{-1}. The relatively large D that we obtained for excitons in NTs is in good agreement with the large carrier mobility estimated in NTs from electrical transport measurements.[49,50] When using the Einstein relation that connects the diffusion and mobility coefficients, then the mobility extracted from the obtained exciton diffusion is of order 4×10^3 cm^2(V s)$^{-1}$; this favorably compares with the carrier mobility of about 10^4 cm^2(V s)$^{-1}$ that was extracted from transport measurements.[49,50] Moreover, since the exciton lifetime in the annealed film is about 1 ps (Table I), we can also calculate the exciton diffusion length, $L_D=(2D\tau_D)^{1/2}$; we get for excitons in annealed NT $L_D\approx 100$ nm. This relatively long diffusion length may explain why excitons are so susceptible to defects that exist on the NT surface. It can also explain the partial decay of $P(t)$ during the exciton lifetime.

The radius of curvature, R, should not be very different for NTs in the annealed and unannealed films. Thus from the slower $P(t)$ dynamics in the unannealed film we conjecture that D for excitons in unannealed NT films is much smaller than in unannealed films, consistent with the much slower exciton recombination dynamics in these films. R cannot be easily estimated for NTs in solution and thus we cannot use the exciton diffusion model to obtain D in solution. Nevertheless, it is surprising that the polarization memory dynamics is so different for NTs in solution. This shows that excitons in isolated NTs in solution are probably quickly trapped, and this influences their mobility and consequently also their recombination dynamics.

The polarization memory of photogenerated excitons in NTs of all forms is not completely lost within the exciton lifetime. For example, from Fig. 8(a) we estimate the decay time constant of $P(t)$, τ_{PM}, to be about 3 ps for NTs in the annealed film (Table I), whereas the exciton recombination time, τ, is about 1 ps in the same film [Fig. 4(a) and Table I]. The same is true for NTs in solution. Whereas the exciton recombination time τ is about 8 ps with a long tail towards longer times [$\omega_{probe}=0.96$ eV, Fig. 5(a) and Table I], the polarization memory hardly decays up to 60 ps [Fig. 7(a)]. From this discussion we conjecture that if excitons in NTs were radiative, then their fluorescence emission would be polarized.[13] It is therefore not surprising that we measured polarized PL emission from NTs in solution, as shown in Fig. 9. It is apparent that the PL component, $PL_{\parallel}$ with polarization parallel to that of the excitation pump, is stronger than the perpendicular component, $PL_{\perp}$; this is true for all measured wavelengths (Fig. 9). We define the PL polarization degree, P_{PL} for the cw emission as $P_{PL}=(PL_{\parallel}-PL_{\perp})/(PL_{\parallel}+PL_{\perp})$. From the two measured PL components, we calculate P_{PL} spectrum and plotted it in Fig. 9. P_{PL} remains approximately constant at $P^*=0.14$ throughout the measured spectrum, with average fluctuations of the order of 0.03. We note that P_{PL} spectrum does not follow the PL emission spectrum; namely it does not contain the same dips and peaks as in the absorption and PL spectra.

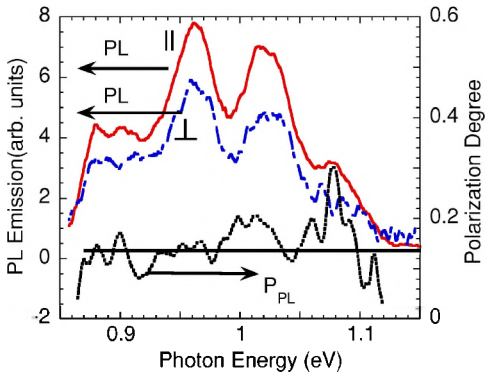

FIG. 9. (Color online) The parallel and perpendicular components (with respect to the pump polarization) of the polarized PL emission spectrum of NTs in solution. The spectrum of the PL polarization degree, P_{PL} (see text) is also shown.

From the average cw PL polarization degree P^* it might be possible to calculate the PL lifetime for NTs in solution. Given that the exciton polarization memory decays with time, and can be extrapolated to reach $P^*=0.14$ at about $t=500$ ps [see Fig. 8(b), for the PB at 0.96 eV], we may estimate the average emission time τ_{PL} from the measured P^*. From $P(t)$ decay we obtain $\tau_{PL}\approx 500\pm 100$ ps for NTs in D_2O solution. Our estimated τ_{PL} is not in disagreement with a more direct measurement of transient PL decay.[14] Using the technique of optical Kerr gating it was measured that PL mostly decays within the first 10 ps, with a very long tail towards longer times. The long tail could not be measured, however, since the optical Kerr gating has a small dynamics range of one order of magnitude for NTs in solution.[14] We note that the obtained τ_{PL} cannot be far off, since otherwise the PL polarization value would have been dramatically different.

The PL emission band is very weak with estimated quantum efficiency, η, of less than 10^{-3}.[8,9] The most careful estimate of η was made in Ref. 14; η was estimated to be 1.7×10^{-4}. In general η is given by the relation[43]

$$\eta=\tau_{nr}/\tau_r, \tag{3}$$

where τ_{nr} is the nonradiative recombination lifetime and τ_r is the radiative recombination lifetime. Some nonradiative re-

combination channels in organic semiconductors include excitons recombination through deep traps, intersystem crossing to the triplet manifold, and excitons dissociation into polarons.[40,51] The PL lifetime τ_{PL} is given in this simple model by the relation[43]

$$1/\tau_{PL} = 1/\tau_{nr} + 1/\tau_r. \quad (4)$$

Using Eqs. (3) and (4) and the values of τ_{PL} and η from above, we calculate τ_{nr}=500 ps, whereas τ_r is estimated to be about 3 μs (with an estimated uncertainty of 2 μs). This relatively long radiative lifetime indicates that excitons in NTs are basically nonradiative; in other words their radiative transitions are almost dipole forbidden.[23] This important conclusion should be taken into account in any electron energy calculation in NTs; this is especially true for models in which electron-hole interaction is explicitly included in the calculations.[20–23]

IV. CONCLUSIONS

The present work reemphasizes that the primary excitations in *S*-NT are excitons, rather than free carriers in continuum bands. This conclusion is based on (1) the photomodulation spectrum where the PA and PB bands are correlated to each other, (2) the existence of polarization memory and its decay, and (3) the similarity between the PL emission, absorption, and PB spectra of NTs in D_2O solution.

We studied the ultrafast exciton recombination and polarization memory dynamics in single-walled NTs of different forms, such as annealed and unannealed films and isolated NTs in D_2O solution. We found that the exciton response kinetics depends on the NT's environment. When the NT is relatively free of surfactant and defects, then the induced disorder is small and the exciton dynamics are fast, of the order of 1 ps. The exciton response dynamics in unannealed films and NTs in D_2O solution are much slower, and this is probably caused by shallow traps in the gap that are introduced by structural defects and impurities on the NT surface; these traps slow down the exciton kinetics. Also, M-NT may enhance the energy relaxation rate in SWCNT films, where S-NT and M-NT are bundled together. The shallow traps are manifested by (*i*) slower exciton diffusion towards recombination centers, which reduces the recombination rate, and (*ii*) a slower rate for the exciton polarization memory decay. From the polarization memory decay in the annealed film we could extract the exciton diffusion constant, D, and diffusion length, L_D, using the "exciton diffusion around the corner model", which is associated with the NT radius of curvature. For annealed films we obtained $D \approx 100$ cm^2 s^{-1}, and $L_D \approx 100$ nm.

We also measured polarized PL emission in NTs in D_2O solution with bands that follow the absorption subbands. We found that the average PL polarization degree P^* is constant at 0.14 across the PL spectrum. From the value of P^* and the exciton polarization memory decay dynamics for NT in solution we estimated the PL lifetime in NT to be about 500 ps. From this relatively long PL lifetime coupled with the minute PL emission quantum efficiency, we estimated the radiative transition time in NT to be of the order of 3±2 μs.

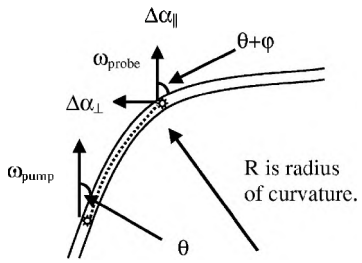

FIG. 10. Schematic representation of the time-dependent pump and probe polarizations, excitons diffusion and polarization, and the geometrical relationship between the three.

ACKNOWLEDGMENTS

This work was supported in part by the NSF (DMR 02-02790) and a grant in aid from the University of Utah. At the University of Texas at Dallas, the work was supported by DARPA Grant No. MDA 972-02-C-005 and the Robert A. Welch foundation.

APPENDIX: POLARIZATION MEMORY: THE "EXCITON DIFFUSION AROUND THE CORNER" MODEL

When polarized light pulses are resonantly absorbed by the medium, the consequent photoexcitations may have distinct polarization, which may exist for longer time than the pulse duration. Since NTs are considered to be quasi-1D, and the excitons localized along the NTs with a wave-function extent of few nm,[18,20–23] then polarization memory (PM) is initially photogenerated. The polarization memory can subsequently decay in isolated NTs when the photogenerated exciton diffuses along a bent NT so that its direction becomes random with respect to the polarization of the pump pulse that causes its generation. A similar model was used before to obtain soliton diffusion in $t-(CH)_x$.[48]

We consider that in SWCNT film the NTs are randomly oriented in two dimensions. Following light absorption by a NT, an exciton with its dipole moment along the NT orientation is photogenerated. In addition, we also consider that each NT has a radius of curvature R (Fig. 10). Two pulses are involved in the transient PM measurements. The pump pulse with a linear polarization and the probe pulse with its polarization is either parallel (∥) or perpendicular (⊥) to that of the pump pulse (Fig. 10). We define θ as the initial angle between the pump polarization and the NT principal direction. At time t after excitation the photogenerated exciton diffuses along the bent NT to a position forming an angle φ respect to its initial position. At that time the angle between the pump polarization and the NT principal direction becomes $(\theta+\varphi)$ (Fig. 10). Consequently the angle between the probe polarization and the direction of the exciton dipole moment on the NT for the parallel pump/probe polarization configuration is thus $(\theta+\varphi)$, whereas the angle is $(90^\circ+\theta+\varphi)$ for the perpendicular pump/probe configuration.

We can now calculate the induced absorption, $\Delta\alpha$, assuming that it is a $\chi^{(3)}$ process for the probe parallel ($\|$) and perpendicular ($\perp$) to the pump polarization, respectively, at time t, averaged over the random NT orientation in 2D:

$$\Delta\alpha_{\|}(\varphi) = c\int \cos^2\theta\cos^2(\theta+\varphi)d\theta = \frac{c\pi}{4}(3\cos^2\varphi+\sin^2\varphi), \tag{A1}$$

$$\Delta\alpha_{\perp}(\varphi) = c\int \cos^2\theta\sin^2(\theta+\varphi)d\theta = \frac{c\pi}{4}(\cos^2\varphi+3\sin^2\varphi). \tag{A2}$$

The polarization memory is defined as

$$P(\varphi) = \frac{\Delta\alpha_{\|}(\varphi)-\Delta\alpha_{\perp}(\varphi)}{\Delta\alpha_{\|}(\varphi)+\Delta\alpha_{\perp}(\varphi)} = \frac{1}{2}\cos(2\varphi). \tag{A3}$$

During the exciton diffusion motion we assume that the angle φ follows a Gaussian distribution because of the random diffusion process.[22] The obtained polarization memory P must therefore be averaged over the Gaussian distribution:

$$\langle P(\varphi)\rangle = \int \frac{1}{2}\cos(2\varphi)\frac{1}{\sqrt{2\pi\langle\varphi^2\rangle}}\exp\left(-\frac{\varphi^2}{2\langle\varphi^2\rangle}\right)d\varphi = \frac{1}{2}\exp(-2\langle\varphi^2\rangle). \tag{A4}$$

Here we took the average angle $\varphi=0$ at $t=0$ because we assume that the NT orientation is random; however, the average of φ^2 cannot be zero due of the NT curvature.

To calculate the average angle $\varphi(t)$ we use the geometrical relation $\varphi(t)=L(t)/R$, where $L(t)$ is the diffusion length along the NT, which can be calculated using the relation $L(t)=(2Dt)^{1/2}$, and D is the diffusion constant. We thus obtain

$$P(t) = p(0)\exp\left(-\frac{4D}{R^2}t\right), \tag{A5}$$

which we used to estimated the diffusion constant D from the measured $P(t)$ in the text.

*To whom correspondence should be addressed; e-mail: val@physics.utah.edu

[1] A. B. Dalton, S. Collins, E. Munoz, J. M. Razal, V. H. Ebron, J. P. Ferraris, J. N. Coleman, B. G. Kim, and R. H. Baughman, Nature (London) **423**, 703 (2003).

[2] P. G. Collins, A. Zettl, H. Bando, A. Thess, and R. E. Smalley, Science **278**, 100 (1997).

[3] R. Saito, G. Dresselhaus, and M. S. Dresselhaus, *Physical Properties of Carbon Nanotubes* (Imperial College Press, London, 1999).

[4] Z. M. Li, Z. K. Tang, H. J. Liu, N. Wang, C. T. Chan, R. Saito, S. Okada, G. D. Li, J. S. Chen, N. Nagasawa, and S. Tsuda, Phys. Rev. Lett. **87**, 127401 (2001).

[5] W. Z. Liang, G. H. Chen, Z. M. Li, and Z. K. Tang, Appl. Phys. Lett. **80**, 3415 (2002).

[6] G. S. Duesberg, I. Loa, M. Burghard, K. Syasssen, and S. Roth, Phys. Rev. Lett. **85**, 5436 (2000).

[7] A. Hartschuh, H. N. Pedrosa, L. Novotny, and T. D. Krauss, Science **301**, 1354 (2003).

[8] M. J. O'Connell, S. M. Bachilo, C. B. Huffman, V. C. Moore, M. S. Strana, E. H. Haroz, K. L. Rialon, P. J. Boul, W. H. Noon, C. Kittrell, J. P. Ma, R. H. Hauge, R. B. Weisman, and R. E. Smalley, Science **297**, 593 (2002).

[9] S. M. Bachilo, M. S. Strano, C. Kittrell, R. H. Hauge, R. E. Smalley, and R. B. Wiesman, Science **298**, 2361 (2002).

[10] J. Lefebvre, Y. Homma, and P. Finnie, Phys. Rev. Lett. **90**, 217401 (2003).

[11] J. A. Misewich, R. Martel, Ph. Avouris, J. C. Tsang, S. Heinze, and J. Tersoff, Science **300**, 783 (2003).

[12] M. Freitag, J. Chen, J. Tersoff, J. C. Tsang, Q. Fu, J. Liu, and Ph. Avouris, Phys. Rev. Lett. **93**, 076803 (2004).

[13] J. Lefebvre, J. M. Fraser, P. Finnie, and Y. Homma, Phys. Rev. B **69**, 075403 (2004).

[14] F. Wang, G. Dukovic, L. E. Brus, and T. F. Heinz, Phys. Rev. Lett. **92**, 177401 (2004).

[15] T. Ando, J. Phys. Soc. Jpn. **66**, 1066 (1997).

[16] M. Ichida, S. Mizuno, Y. Tani, Y. Saito, and A. Nakamura, J. Phys. Soc. Jpn. **68**, 3131 (1999).

[17] C. L. Kane and E. J. Mele, Phys. Rev. Lett. **90**, 207401 (2003).

[18] T. G. Pedersen, Phys. Rev. B **67**, 073401 (2003).

[19] M. Ichida, S. Mizuno, Y. Saito, H. Kataura, Y. Achiba, and A. Nakamura, Phys. Rev. B **65**, 241407 (2002).

[20] C. D. Spataru, S. Ismail-Beigi, L. X. Benetict, and S. G. Louie, Phys. Rev. Lett. **92**, 077402 (2004).

[21] E. Chang, G. Bussi, A. Ruini, and E. Molinari, Phys. Rev. Lett. **92**, 196401 (2004).

[22] V. Perebeinos, J. Tersoff, and Ph. Avouris, Phys. Rev. Lett. **92**, 257402 (2004).

[23] H. Zhao and S. Mazumdar, Phys. Rev. Lett. **93**, 157402 (2004).

[24] M. Chandross and S. Mazumdar, Phys. Rev. B **55**, 1497 (1997).

[25] M. J. Rice and Y. N. Gartstein, Phys. Rev. Lett. **73**, 2504 (1994).

[26] A. Race, W. Barford, and R. J. Bursill, Phys. Rev. B **64**, 035208 (2001).

[27] T. Hertel and G. Moos, Chem. Phys. Lett. **320**, 359 (2000); Phys. Rev. Lett. **84**, 5002 (2000).

[28] Y. C. Chen, N. R. Raravikar, L. S. Schadler, P. M. Ajayan, Y. P. Zhao, T. M. Lu, G. C. Wang, and X. C. Zhang, Appl. Phys. Lett. **81**, 975 (2002).

[29] S. Tatsuura, M. Furuki, Y. Sato, I. Iwasa, M. Tian, and H. Mitsu, Adv. Mater. (Weinheim, Ger.) **15**, 534 (2003).

[30] J. S. Lauret, C. Voisin, G. Cassabois, C. Delalande, Ph. Roussignol, O. Jost, and L. Capes, Phys. Rev. Lett. **90**, 057404 (2003).

[31] O. J. Korovyanko, C.-X. Sheng, Z. V. Vardeny, A. B. Dalton, and R. H. Baughman, Phys. Rev. Lett. **92**, 017403 (2004).

[32] G. N. Ostojic, S. Zaric, J. Kono, M. S. Strano, V. C. Moore, R. H. Hauge, and R. E. Smalley, Phys. Rev. Lett. **92**, 117402 (2004).

[33] A. Thess, R. Lee, P. Nikolaev, H. Dai, P. Petit, J. Pobert, C. Xu, Y.

H. Lee, S. G. Kim, A. G. Rinzler, D. T. Colbert, G. E. Scuseria, D. Tomanek, J. E. Fischer, and R. E. Smalley, Science **273**, 483 (1996).
[34] T. V. Sreekumar, T. Liu, S. Kumar, L. M. Ericson, R. H. Hauge, and R. E. Smalley, Chem. Mater. **15**, 175 (2003).
[35] Z. V. Vardeny, J. Strait, D. Moses, T. C. Chung, and A. J. Heeger, Phys. Rev. Lett. **49**, 1657 (1982).
[36] P. Nikolaev, M. J. Bronikowski, K. Bradley, F. Rohmund, D. T. Colbert, K. A. Smith, and R. E. Smalley, Chem. Phys. Lett. **313**, 91 (1999).
[37] G. U. Sumanasekera, C. K. W. Adu, S. Fang, and P. C. Eklund, Phys. Rev. Lett. **85**, 1096 (2000).
[38] M. E. Itkis, S. Niyogi, M. E. Meng, M. A. Hamon, H. Hu, and R. C. Haddon, Nano Lett. **2**, 155 (2002).
[39] T. Pichler, M. Knupfer, M. S. Golden, J. Fink, A. Rinzler, and R. E. Smalley, Phys. Rev. Lett. **80**, 4729 (1998).
[40] S. V. Frolov, M. Liess, P. A. Lane, W. Gellermann, and Z. V. Vardeny, Phys. Rev. Lett. **78**, 4285 (1997).
[41] P. M. Rafilov, H. Jantoljak, and C. Thomsen, Phys. Rev. B **61**, 16 179 (2000).
[42] M. Hulman, W. Plank, and H. Kuzmany, Phys. Rev. B **63**, 081406 (2001).
[43] J. Pankove, *Optical Processes in Semiconductors* (Prentice–Hall, Englewood Cliffs, NJ, 1971).
[44] Z. Vardeny and J. Tauc, *Semiconductors Probed by Ultrafast Laser Spectroscopy*, edited by R. R. Alfano (Academic, Orlando, FL, 1984), Vol. 2, p. 23.
[45] Z. Vardeny, J. Strait, and J. Tauc, Appl. Phys. Lett. **42**, 580 (1983).
[46] R. A. Cheville and N. J. Halas, Phys. Rev. B **45**, R4548 (1992).
[47] Z. Vardeny, P. O'Connor, S. Ray, and J. Tauc, Phys. Rev. Lett. **44**, 1267 (1980).
[48] Z. Vardeny, J. Strait, D. Pfost, J. Tauc, and B. Abeles, Phys. Rev. Lett. **48**, 1132 (1982).
[49] M. Bockrath, D. H. Cobden, P. L. McEuen, N. G. Chopra, A. Zettl, A. Thess, and R. E. Smalley, Science **275**, 1922 (1997).
[50] N. R. Franklin, Q. Wang, T. W. Tombler, A. Javey, M. Shim, and H. Dai, Appl. Phys. Lett. **81**, 913 (2002).
[51] M. Wohlgenannt, W. Graupner, G. Leising, and Z. V. Vardeny, Phys. Rev. B **60**, 5321 (1999).